Analysis of Voltage Distribution in Transformer Windings During Circuit Breaker Prestrike

M. Popov, R.P.P. Smeets, L. van der Sluis, H. de Herdt and J. Declercq

***Abstract* - In this work, the circuit breaker prestrike effect that occurs during energizing a distribution transformer is investigated. An experimental test setup that consists of a supply transformer, a vacuum circuit breaker (VCB), a cable and a test transformer is built, and prestrikes in the VCB are recorded. The test transformer is a prototype distribution transformer, with installed measuring points along transformer windings in each phase. The transformer is modeled by lumped parameters extracted from telegrapher's equations in discrete form.**

Voltage oscillations during switching-in operations are recorded and calculated with and without a cable installed between the VCB and the transformer. Computed voltages show good agreement with the measured voltages. Described method can be used by transformer manufacturers to estimate voltage wave forms during switching or lightning, and to provide useful information for insulation coordination studies

***Keywords*: transformer, circuit breaker, switching-in, prestrikes, oscillations.**

I. Introduction

IT is well known that during switching highly inductive loads like transformers and motors, under specific conditions multiple restrikes in the circuit breaker can occur. Multiple restrikes are fast voltage surges which proceed along the cable and reach the transformer or motor terminals. Because of different surge impedances at terminals, a wave reflection and absorption takes place. Voltage oscillations which proceed toward windings are continuously superposed by new voltage waves from new upcoming surges. Hence, voltage waveforms along the transformer winding within a particular time interval can have very different amplitude and rate of rise. Their oscillations contain a broad frequency range which can be from a few kilohertz up to a few megahertz. These are unwanted phenomena which cause deterioration and failure of the equipment insulation. Almost one third of all motor failures occur because of fast switching surges [1]. Switching surges which enter the windings are non-linearly distributed [2]. Besides, sometimes high inter-turn overvoltages can take place which stress the thin insulation and accelerate its failure. So far, a lot of work has been done on transformer and motor switching [3-9]. However, voltage transients are measured on transformer terminals and prediction of the voltage distribution along the windings is difficult to be done. In [10] a computer model for motor windings is described which is applied during sequential pole closing [11]. It is also applied for determination of inter-turn voltages during energizing a motor with a VCB [12].
Most of the time, the geometry of the windings and dimensions are not known. Furthermore, a proper model based on transformer geometry and type of windings is difficult to develop. Consideration of the frequency-dependent losses is another problem.

So far, there was successful work done on transformer modeling. In [13, 14], a hybrid model based on transmission line theory was successfully applied to describe the wave propagation in large shell-type transformers. An accurate approach for modeling transformers and motors is done by applying the so called vector fitting [15]. This model is based on the measured frequency admittance matrix of the transformer, the elements of which are admittances measured from any provided measuring point in the transformer windings [16]. The advantage of the latter model is that it gives the possibility to use existing simulation software like EMTP.

In this work, the prestrike effect during energizing the transformer was investigated. Voltage waveforms on transformer terminals are measured and they are used as an input parameter to the transformer model. A lumped-parameter model based on discretized telegraphist's equations is applied [17]. It was found that this approach can be successfully applied for computation of voltages along the windings, even for matrices with large dimensions (100x100). Computations are done in frequency domain, and time domain solutions are provided by applying inverse continuous Fourier transform [18]. Measurements and computations are also done with and without applying a cable between the VCB and transformer. The computations are verified by laboratory measurements.

This work was financially supported by the Dutch Scientific Foundation NWO/STW under Grant VENI, DET.6526.

M. Popov and L. van der Sluis are with the Delft University of Technology, Faculty of Electrical Engineering, Mathematics and Informatics, Mekelweg 4, Delft 2628CD, The Netherlands, (e-mail: M.Popov@tudelft.nl).

R.P.P.Smeets is with KEMA, 6800 ET Arnhem and Department of Electrical Engineering, Eindhoven University of Technology, Eindhoven, 5600 MB, The Netherlands (e-mail: Rene.Smeets@kema.com).

H. de Herdt and J. Declercq are with Pauwels Trafo Belgium N.V., Antwerpsesteenweg 167, B-2800 Mechelen, Belgium (e-mail: Hans.de.Herdt@pauwels.com, JDeclercq@HansenTransmissions.com).

Paper submitted to the International Conference on Power Systems Transients (IPST2009) in Kyoto, Japan June 3-6, 2009

II. Test Transformer and its Representation

A. Transformer description

The test transformer is shown in Fig. 1 . This is a three-phase layer-type transformer. However, the computation and measurements of the voltages along the windings are done per phase whilst other two phases are not connected to the studied phase.

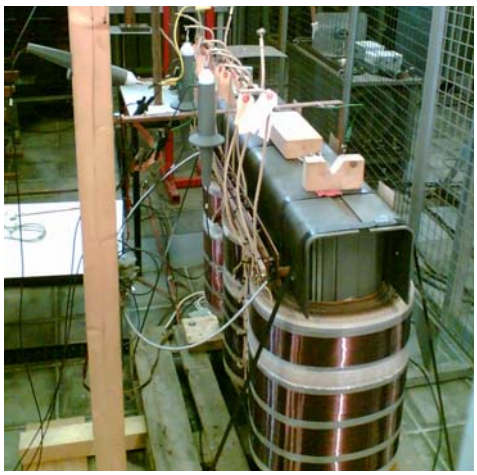

Fig. 1. Test transformer.

The primary transformer winding consists of layers with approximately 140 turns. The transformer is equipped with special measuring points in each phase. In phase A, measuring points are installed at the 3rd and the 5th turn. In phase B, the measuring points are at the 290th and the 580th turn, and in phase C, the measuring points are at the 444th and the 888th turn. All measuring points can be directly reached as it can be seen from Fig. 1. The most important parameters of the transformer are summarized in Table I.

TABLE I
Transformer Data

Transformer Power	630 kVA
Transformer ratio	15375 V / 400 V
No-load losses	770 W
No-load current	0.3 %
Number of layers (HV side)	10
Number of turns in a layer	~ 140
Inner radius of HV winding	135.3 mm
External radius of HV winding	163.3 mm
Inner radius of the LV winding	97 mm
Wire diameter	3.0 mm
Double wire insulation	0.1 mm
Distance between layers	0.4 mm
Coil's height	425 mm

B. Transformer representation

Studied transformer is a layer-type prototype transformer particularly produced for this research. The transformer has measuring points installed in each phase. The tank and the oil are removed so that an easy access to the windings can be provided. The transformer with capacitances and inductances is represented in Fig. 2. The inductance matrix is formed by the self inductances of a group of turns and mutual inductances between the turns. The capacitance matrix is formed by capacitances between layers and capacitances from the top and the bottom of the layers to the transformer tank.

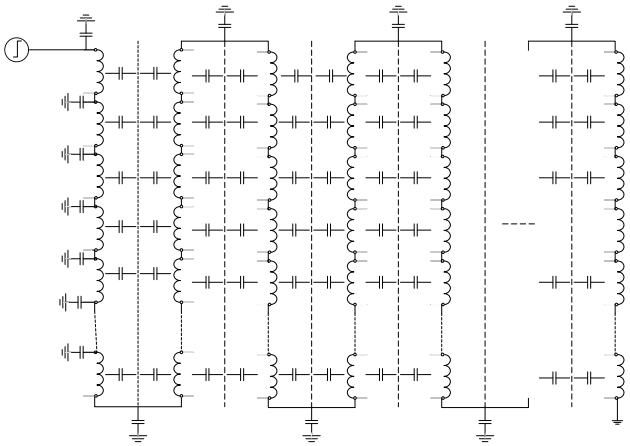

Fig. 2. Transformer capacitances and inductances

The transformer represented in Fig. 2 can be simplified by re-arranging the capacitances. To do this, we will consider an equipotential surface between the layers [2]. In this way, one can divide a group of winding in the following way. Half of the capacitance between coils is added to the edges of the coils [19-21]. Then, it is assumed that there is an equipotential line in the middle of the coil, so that the capacitance between coils can be added as a cross-over capacitance at each coil with a value equal to the half of the value of the total capacitance. The description is given in Fig. 3.

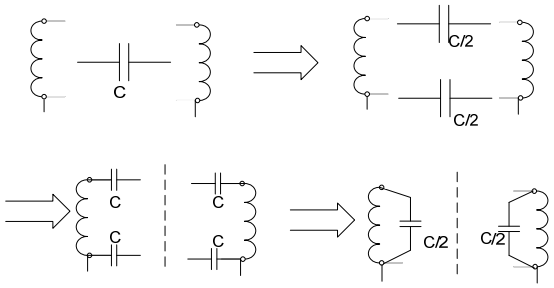

Fig. 3. Simplification of a section of the transformer.

Fig. 4 is the final model of the transformer. It has to be pointed out that the cross-over capacitances which belong to the first and last layer are a half of the cross-over capacitance of the other layers. Capacitances to ground in this case are small because the surface of the top and bottom of the coil is small. They are estimated as less than 1 pF.

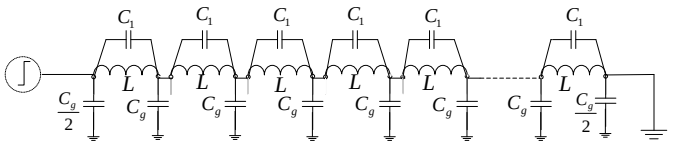

Fig. 4. Final lumped-parameter model for transformer voltage distribution studies

C. Inductance and capacitance matrix

Inductances are calculated by the well known Maxwell formulas on a turn-to-turn basis [22]. The **L** matrix is formed in a way that diagonal elements of the matrix correspond to a group of turns. The off-diagonal elements are mutual inductances between different groups of turns. For simplicity in this case, the number of turns in a group is kept constant. The studied transformer has 10 layers with approximately 142 turns per layer. Each layer is divided in 10 groups with 14 turns per group. So, we assume that a layer consists of 10 groups. So the transformer **L** matrix is of order 100x100. The capacitance matrix is built on a node-to-node basis and because the number of nodes N=B+1 where B is the number of branches represented by inductances, the capacitance matrix is of order 101x101.

Finally, by making use of the inductance matrix **L** and the capacitance matrix **C,** impedance and admittance matrices $\underline{\mathbf{Z}}$ and $\underline{\mathbf{Y}}$ are determined [22]:

$$\underline{\mathbf{Z}} = \left(j\omega + \sqrt{\frac{2\omega}{\sigma\mu_0 d^2}} \right)\mathbf{L} \qquad (1)$$

$$\underline{\mathbf{Y}} = \left(j\omega + \omega \tan\delta \right)\mathbf{C}$$

where

d - is the distance between layers,

σ - is the conductor conductivity,

$\tan\delta$ - is the loss tangent of the insulation.

III. Transformer Modeling

According to [17], a general representation of N-winding transformer can be done by discretizing the transmission line equations. The general govern equations for the voltages and currents are:

$$\frac{dV_i(x)}{dx} = \sum_{j=1}^{N} -\int_0^{\lambda_j} Z_{ij}(x,\beta) I_j(\beta) \quad i=1, 2,\ldots N \qquad (2)$$

$$\frac{dI_i(x)}{dx} = \sum_{j=1}^{N} -\int_0^{\lambda_j} Y_{ij}(x,\beta) V_j(\beta) \quad i=1, 2,\ldots N \qquad (3)$$

Equations (2) and (3) are general equations that represent N-winding transformer model. In (2), $I_j(\beta)$ is the inductive current at a distance β down the jth winding, and $Z_{jj}(x,b)$ is a mutual impedance function. The self- and mutual impedance is frequency dependent, equation (2) is also in frequency domain, so the $V_i(x)$ and $I_j(\beta)$ are Fourier transformer of $V_i(x,t)$ and $I_j(\beta,t)$ respectively. λ_j represents the length of the jth winding. Because we are dealing with only one winding, the computation can be rather simplified, so the solution can be represented in a matrix form:

$$\begin{bmatrix} \mathbf{I_B} \\ \mathbf{V'} \end{bmatrix} = \begin{bmatrix} \mathbf{A} & \mathbf{B} \\ \mathbf{C} & \mathbf{D} \end{bmatrix} \begin{bmatrix} \mathbf{V_B} \\ \mathbf{V'} \end{bmatrix} \qquad (4)$$

where $\mathbf{V_B}$ represents the set of voltages at the winding terminals, and $\mathbf{I_B}$ represents the set of currents entering them:

$$\mathbf{V_B} = \begin{bmatrix} \mathbf{V_S} \\ \mathbf{V_R} \end{bmatrix}, \quad \mathbf{I_B} = \begin{bmatrix} \mathbf{I_S} \\ -\mathbf{I}_R \end{bmatrix} \qquad (5)$$

Applying equation (5), one can calculate the voltages in the internal nodes as:

$$\mathbf{V'} = \left(1 - \mathbf{D}\right)^{-1} \mathbf{C}\mathbf{V_B} \qquad (6)$$

More about derivation of (6) and corresponding submatrices **A**, **B**, **C** and **D** can be found in [17]. The time domain solutions are calculated by continuous inverse Fourier transform [18].

A. Model Verification

The model has been verified by applying it on the circuit shown in Fig. 5. We have to point out that this circuit is not the analyzed transformer circuit to which the described methodology will be applied. Circuit in Fig. 5 is energised by a unit step function. The data are chosen from [17] and in this way the validity of the model is shown. The parameters of the lossless circuit are: L_{kk}=0.27 H, k=1,2,…,6. Mutual inductances between sections: L_{12}= L_{23}= L_{34}= L_{45}= L_{56}=0.255 H, L_{13}= L_{24}= L_{35}= L_{46}=0.235 H, L_{14}= L_{25}= L_{36}=0.216 H, L_{15}= L_{26}=0.199 H, L_{16}=0.183 H. Series capacitance per section is C_1=400 pF and shunt capacitance per section is C_0 =400 pF.

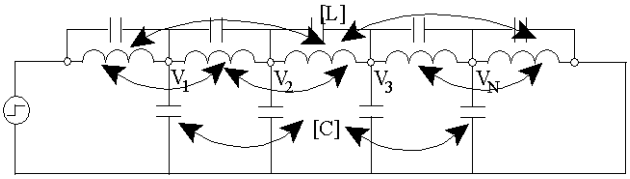

Fig. 5. Equivalent circuit of a transformer winding

Fig. 6 through Fig. 8 present the results of the computation. Fig. 6 presents the numerical results obtained by (6). Fig. 7 presents the ATP-EMTP simulations used to verify the results.

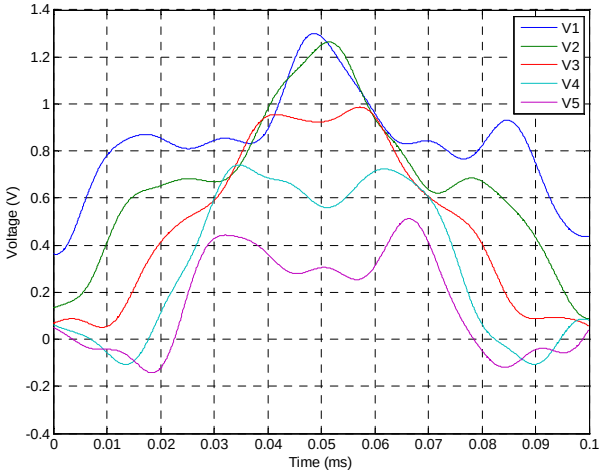

Fig. 6. Computed voltages applying the modal analysis

This is done because the circuit is small and the matrix can be easily modelled by making use of the coupled sections. The problem can be further resolved analytically and these results

are shown in Fig. 8. It can be seen that there is a good agreement between the all results so the way of representation the transformer winding can be done successfully.

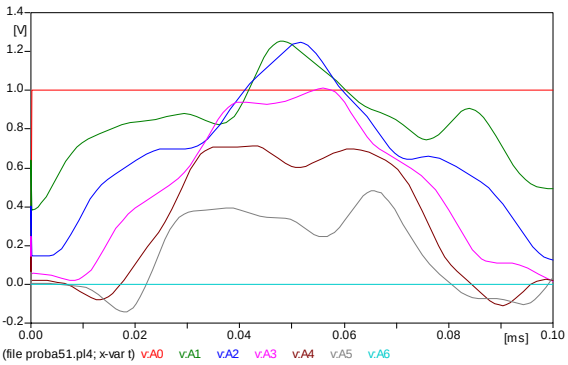

Fig. 7. Computed voltages by ATP-EMTP by taking into account the mutual inductances

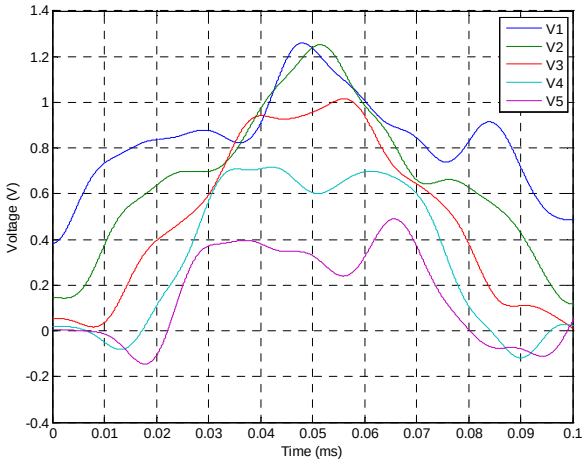

Fig. 8. Accurate analytical solution of the problem

IV. Description of the Measuring Setup

The measuring setup is done similar to the motor switching test circuit IEC 62271-110 [23]. The supply transformer is a special laboratory transformer with a voltage ratio 0.5/100 kV and nominal power of 50 kVA. Because the nominal current is 0.5 A, only switching-in tests at different voltage levels and at low current are performed. A 30 kΩ resistor on the high-voltage transformer side is installed to limit the load current and protect the transformer from high currents. So, the circuit is realized in a way to produce negligible current. The transformer switching test circuit is shown in Fig. 9.

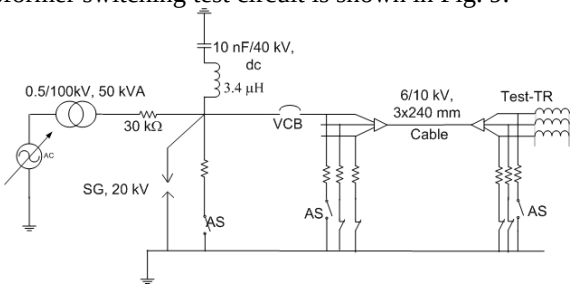

Fig. 9. Transformer switching test circuit.

During switching, a prestrike effect in the VCB takes place, so surges propagate along the cable and reach the transformer windings. The voltages are measured at the transformer terminal and at the measuring points installed along the winding. Voltages are measured by applying 20 kV PMK voltage probes between a specific measuring point and the ground, and currents are measured by a high frequency Pearson Electronic current probe. Both, currents and voltages are recorded by a 4-channel Nicolet Genesis transient recorder with a resolution of 14 bits and a sampling rate of 100 MS/s.

V. Test Results

A. VCB switching-in test

Switching tests with the vacuum circuit breaker are done at different voltage levels. The voltage is changed between 4 kV and 12 kV with a step of 2 kV. Furthermore, measurements are done with and without a cable. As explained in chapter II.C, each layer is divided in 10 sections. Because the total number of turns in a layer is 140, by applying the described model from chapter III, the voltages at the end of sections can be calculated. Therefore, in the analysis in this chapter the measurements and computations do not correspond to the same number of turn. Fig. 10 through Fig. 13 shows the results for the case when the transformer phase B is energized by supply voltage of 6 kV and 8 kV.

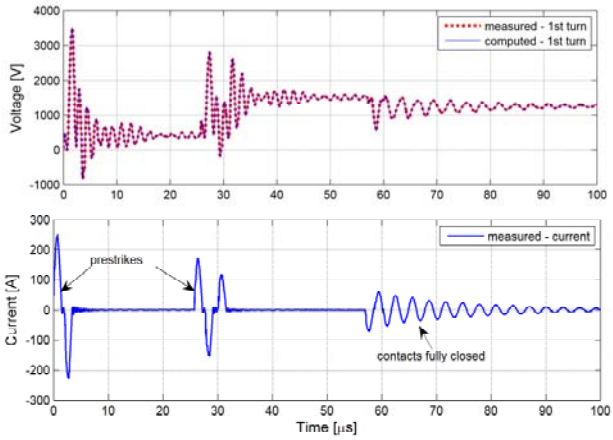

Fig. 10. Measured and computed transformer terminal voltage in phase B during transformer energizing with applied voltage of 6 kV (upper Figure); measured circuit breaker current (lower Figure).

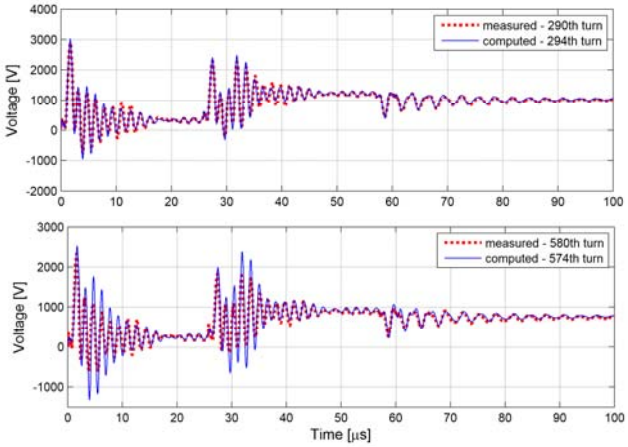

Fig. 11. Measured and computed voltages at specific turns in phase B during transformer energizing with applied voltage of 6 kV.

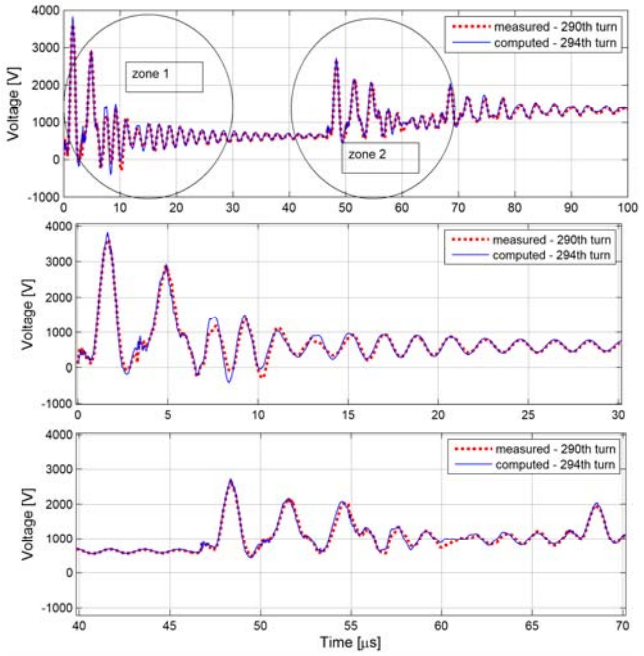

Fig. 12. Measured and computed voltages in phase B during transformer energizing with applied voltage of 8 kV (upper Figure); zone 1, first 30 μs (middle Figure); zone 2, 40 - 70 μs (lower Figure).

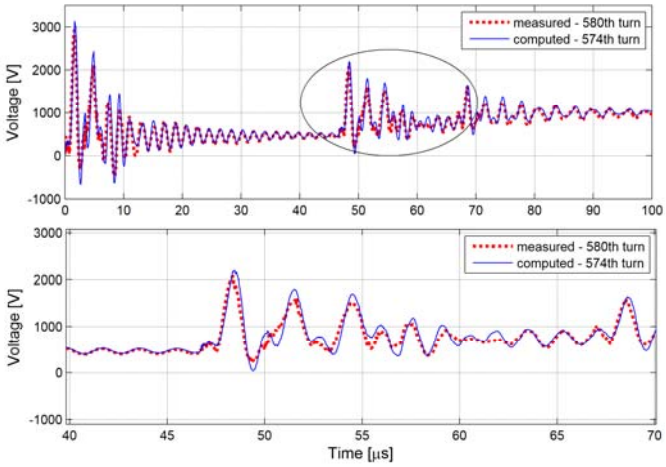

Fig. 13. Measured and computed voltages in phase B for transformer energizing with applied voltage of 8 kV (upper Figure); increased time scale between 40 - 70 μs (lower Figure).

During energizing the transformer, a prestrike occurs before the contacts physically touch each other. Fig. 10 shows the first test done with a supply voltage of 6 kV. This test is followed by two prestrikes. After approximately 25 μs from the second prestrike, the contacts fully close and the load current is established. Fig. 11 shows measured and computed voltages at specific points during 6 kV transformer energizing. The next test is done with a supply voltage of 8 kV as shown in Fig. 12. In this case, two prestrikes can be seen just as in the previous case, and the duration of the prestrike current is longer. This is according to the expectations that, the higher the system voltage, the higher the duration of the prestrikes.

The oscillation frequency of the prestrike current is about 280 kHz. This frequency normally depends on the source side equivalent capacitance, load side equivalent capacitance and cable inductance [8]. The amplitude of the current during second prestrike, as can be seen from Fig. 10 has lower value than that during the first prestrike. The reason for this is that the prestrike current depends on the withstand voltage between the circuit breaker contacts. Prestrike occurs when the transient recovery voltage is greater than the withstand voltage. As the contacts approach to each other, the withstand voltage is lower and the prestrike current decreases accordingly. In all Figures, measured and computed voltages are represented. For the turn 1 which is the terminal transformer voltage, there is a very good matching. From the measured voltage, a numerical Fourier transform is done. The computed result is the inverse Fourier transform, which shows that the time domain solution is correctly obtained.

This is important because the measured voltage at the transformer terminal is an input parameter for the determination of the voltage distribution in all windings. Furthermore, it can be seen that there is a good agreement between measured and computed voltages.

Fig. 12 presents the measured and computed voltages for the second test with supply voltage of 8 kV in phase B. Voltage transients in the 290th turn are measured and compared with the computed transients in the 294th turn. Fig. 13 shows the enlarged time scale for the zone 2 at 580th turn.

In Fig. 14, the results of a switching test without a cable between the VCB and transformer are presented for a supply voltage of 8 kV.

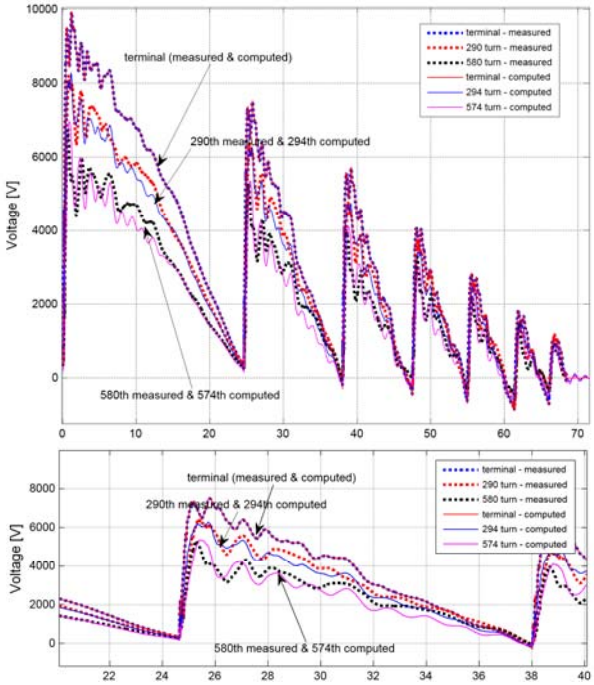

Fig. 14. Measured and computed voltages in phase B (upper Figure); increased time scale (middle Figure); source voltage is 8 kV.

Solid lines represent the computed results, whilst interrupted lines show the measured results. The prestrike is damped rapidly, and the voltage decreases rapidly after arc extinction.

The reason for this is that the load voltage side capacitance is very low and consists only of the transformer bushing capacitance and busbar capacitance that connects the circuit breaker and transformer. This implies that the voltage escalates more than in the case when a cable between the

transformer and the VCB is connected. Furthermore, in all cases it can be seen that the voltage when a cable is applied, is about the half of the voltage value when no cable between the VCB and the transformer is applied. This is because the voltage is divided between the cable and the transformer.

VI. Conclusion

In this paper, the influence of the prestrike in the circuit breaker on the transformer was investigated. From the results, it can be seen that the case when a cable exists is different from that when no cable exists. The cable contributes to longer frequency oscillations and lower voltage amplitudes, whilst switching the transformer without cable will contribute to steeper voltage rise and short duration of the restrike current. This work shows that the lumped-parameter model based on discrete telegraphist's equations can be used with full success to study voltage transients along transformer windings. The modeling needs only information about the geometrical dimensions of the transformer which can be easily obtained by the manufacturer. The applied model is general and applicable for the analysis of voltage distributions in transformer windings during lightning surges. It can also be applied for transformer switching off studies.

VII. References

[1] B.K.Gupta, E.P.Dick, A. Greenwood, M. Kurtz, T.S. Lauber, B.A. Lloyd, A. Narang, P.R. Pillai, G.C. Stone: "*Turn Insulation Capability of Large AC motors: Vol. 2, Appendixes: Final Report*", Technical Report, EPRI-EL-5862-Vol.2, 1988.

[2] G. Stein: "A Study of the Initial Surge Distribution in Concentric Transformer Windings", *AIEE Transaction*, September 1964, pp. 877-892.

[3] G.C. Damstra: "Virtual Chopping Phenomena Switching Three-Phase Inductive Circuits", *Colloquium of CIGRE SC 13*, Helsinki, September 1981.

[4] W.M.C. van den Heuvel, J.E. Daalder: "*Interruption of a Dry Type Transformer in No-load by a Vacuum Circuit Breaker"*, EUT Report, Eindhoven, 1983, ISBN 90-6144-141-2.

[5] A.O. Soysal: "Protection of Arc Furnace Supply Systems From Switching Surges", Proceedings of 1999 *IEEE PES Winter Meeting*, 31 January-4 February 1999, New York, NY, Vol. 2, pp. 1092-1095, ISBN 0-7803-4893-1.

[6] J. Kosmac, P. Zunko: "A Statistical Vacuum Circuit Breaker Model for Simulation of Transient Overvoltages", *IEEE Transactions on Power Delivery*, Vol. 10, No. 1, January 1995, pp. 294-300.

[7] Cigre SC A3: "*Electrical Environment of Transformers – Impact of Fast Transients"*, Summary Paper of the CIGRE JWG 12/32/23.21, A3-04 (SC) 26 IWD.

[8] M. Popov, L. van der Sluis, G. C. Paap: "Investigation of the Circuit Breaker Reignition Overvoltages Caused by No-load Transformer Switching Surges", *European Transactions on Electric Power* (*ETEP*), Vol. 11, No. 6, November/December 2001, pp. 413-422.

[9] E. Colombo, G. Costa, L. Piccarreta: "Results of an Investigation on the Overvoltages due to a Vacuum Circuit Breaker When Switching an H.V. Motor", *IEEE Transactions on Power Delivery*, Vol. 3, No. 1, January 1988, pp. 205-213.

[10] J.L.Guardado, K.J. Cornick: "A Computer Model for Calculating Steep-Fronted Surge Distribution in Machine Windings", *IEEE Transaction on Energy Conversion*, Vol. 4, No.1, March 1989, pp. 95-101.

[11] J.L. Guardado, V. Venegaz, E. Melgoza, K.J. Cornick, J.L. Naredo: "Transient Overvoltages in Electrical Motors During Sequential Pole Closure", *IEEE Transaction on Energy Conversion*, Vol.14, No.4, December 1999, pp. 1057-1064.

[12] J.L. Guardado, V. Carrillo, K.J. Cornick: "Calculation of Interturn Voltages in Machine Windings During Switching Transients Measured on Terminals", *IEEE Transaction on Energy Conversion*, Vol.10, No.1, March 1995, pp. 87-94.

[13] Y. Shibuya, S. Fujita, N. Hosokawa: "Analysis of Very Fast Transient Overvoltages in Transformer Winding", *IEE Proceedings on Generation Transmission and Distribution*, Vol.144, No. 5, September 1997, pp.461-468.

[14] M. Popov, L. van der Sluis, G.C. Paap, H. de Herdt: "Computation of Very Fast Transient Overvoltages in Transformer Windings", *IEEE Transactions on Power Delivery*, Vol. 18, No. 4, October 2003, pp. 1268-1274.

[15] B. Gustavsen, A. Semlyen: "Rational Approximation of Frequency Domain Responses by Vector Fitting", *IEEE Transactions on Power Delivery*, Vol. 14, No. 3, July 1999, pp. 1052-1061.

[16] B. Gustavsen: "Computer Code for Rational Approximation of Frequency Dependent Admittance Matrices", *IEEE Transactions on Power Delivery*, Vol. 17, No. 4, October 2002, pp. 1093-1098.

[17] D.J. Wilcox: "Theory of Transformer Modelling Using Modal Analysis", *IEE Proceedings-C*, Vol. 138, No. 2, March 1991, pp.121-128.

[18] J.P. Bickford, N. Mullineux, J.R. Reed: "*Computation of Power System Transients*", IEE, Peter Peregrinus Ltd., 1976, ISBN 0901223859.

[19] R.C. Degeneff, W.J. McNutt, W. Neugebauer, J. Panek, M.E. McCallum, C.C. Honey: "Transformer Response to System Switching Voltage", *IEEE Transactions on Power Apparatus and Systems*, Volume PAS-101, No.6, June 1982, pp. 1457-1470.

[20] W.J. McNutt, T.J. Blalock, R.A. Hinton: "Response of Transformer Windings to System Transient Voltages": *IEEE Transactions on Power Apparatus and Systems*, Vol. PAS-93 (1974), pp. 457-467.

[21] R.C. Dugan. R. Gabrick, J.C. Wright, K.V. Pattern: "Validated Techniques for Modeling Shell-form EHV Transformers", *IEEE Transactions on Power Delivery*, Vol.4, No.2, April 1989, pp. 1070-1078.

[22] Y. Shibuya, S. Fujita: "High Frequency Model of Transformer Winding", *Electrical Engineering in Japan*, Vol. 146, no.3, 2004, pp. 8-15.

[23] IEC 62271-110 *High-voltage switchgear and control gear Part 110*: Inductive load switching.